Magnetic dipole transitions in the $n=3$ level of highly ionized zinc, germanium, and selenium

K. H. Burrell, R. J. Groebner, N. H. Brooks, and L. Rottler
GA Technologies Inc., P.O. Box 85608, San Diego, California 92138
(Received 23 September 1983)

We present measured wavelengths of newly identified magnetic dipole transitions in the Mg I through Cl I sequences in zinc, germanium, and selenium that were excited after these elements were injected into tokamak plasmas in Doublet-III.

I. INTRODUCTION

The relatively long-wavelength magnetic dipole lines in the $n=2$ shell of highly ionized ions from scandium through nickel have been extensively used in tokamak plasmas for measurements of ion temperature, bulk plasma rotation speed, and impurity transport rates.[1-10] Owing to the spatial variation of the electron temperature, a given ionization stage exists in a spatially localized shell in such plasmas, which permits spatially as well as temporally resolved measurements of ion temperature[1-7] and rotation speed.[8-10] These lines are also useful for impurity transport experiments both because of their convenient wavelengths and because the line intensities are independent of electron density and temperature under typical tokamak conditions, which simplifies data analysis. However, in the new generation of tokamaks, the $n=2$ level of elements up through the iron group (nuclear charge $Z=28$) will be stripped over much of the plasma cross section since anticipated electron temperatures are in the neighborhood of 5 keV. Accordingly, one must use heavier elements to utilize the $n=2$ levels to measure conditions in the plasma center. Use of such elements opens up the additional possibility of employing $n=3$ level magnetic dipole transitions for simultaneous measurements in the cooler, outer regions of the plasma. For these reasons and for the advancement of fundamental atomic physics, it is of interest to identify magnetic dipole lines radiated from the $n=3$ shell of ions with $Z \geq 29$.

Over the last year, several groups (including ours) have worked on magnetic dipole lines in the $n=3$ shell of elements between zinc and molybdenum ($29 \leq Z \leq 42$).[10-15] The purpose of this paper is to give more detail on the first measurements of magnetic dipole lines in the $n=3$ shell of germanium[11] as well as to report more completely on our more recent observations with zinc[15] and selenium.

The paper is organized in the following fashion. Experimental technique is discussed in Sec. II. The measured wavelengths are given in Sec. III and the conclusions are given in Sec. IV. Also included in Sec. II is a discussion of the means of line identification, wavelength determination, and error analysis.

II. EXPERIMENTAL METHOD

A. Equipment used

The measurements made for this paper were performed by injecting small amounts of the element under study into Ohmically heated, deuterium plasmas produced in the Doublet-III tokamak. Plasma parameters for this work were a line averaged electron density n_e between 1×10^{13} cm^{-3} and 5×10^{13} cm^{-3} and a central electron temperature T_e between 1.0 keV and 1.5 keV. The impurity element was introduced either via the laser blowoff technique,[16] which was used for zinc, or via injection of a 10-ms-long gas pulse[17] containing the impurity, which was used for germanium and selenium. The latter two elements were part of a gas mixture containing 90 vol% H_2 and 10 vol% of either GeH_4 or H_2Se. Typically, about 10^{17} atoms of the impurity were injected into a plasma containing about 3×10^{21} ions; accordingly, the impurity was at the trace level and did not usually perturb the plasma significantly.

Wavelength measurements were made using the spectrometers on Doublet-III that are usually devoted to Doppler spectroscopy, spatially resolved visible and near ultraviolet spectroscopy, and vacuum ultraviolet (vuv) spectroscopy. The first two are Spex $\frac{3}{4}$-m Czerny-Turner spectrometers while the last is a Minuteman 1-m grazing-incidence instrument.

The Doppler spectrometer contains a 1200-line/mm ruled grating that is blazed for maximum response near 12 000 Å. A typical entrance slit width for this instrument is 150 μm. The spectrometer views the plasma along a major radius through the plasma midplane. Since this instrument was designed for Doppler ion temperature measurements, it has simultaneous multiwavelength capability through its 1024 channel linear detector (see Fig. 1). Typically, this system is operated in fifth order and produces a spectrum covering 100 Å (i.e., 20 Å in the first order) every 25 to 50 ms, depending on operator choice. Owing to its simultaneous multiwavelength detection capability, this system makes the search for new lines quite rapid. The high spectral order used also makes the wavelength measurements quite precise. Although evacuable and equipped with MgF_2-coated optics, the spectrometer was filled with air during the current work. This limited detection capability to lines with wavelength $\lambda \geq 2000$ Å. In addition, the CsTe photocathode in the first image intensifier limited the wavelength range to $\lambda \leq 3000$ Å.

The other Czerny-Turner spectrometer, dubbed the scanning visible spectrometer, is equipped with a 2400-line/mm holographic grating and is usually used with 500-μm entrance and exit slits. It can view Doublet-III through any of the 16 fiber-optic cables which afford

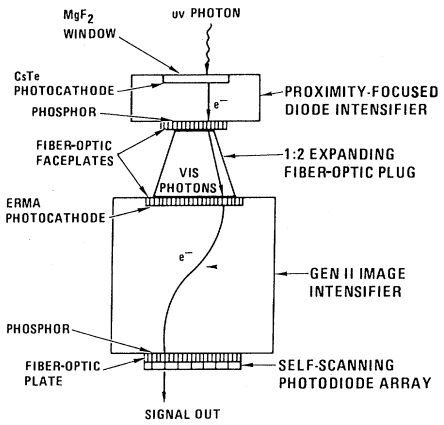

FIG. 1. Drawing of the two-stage image intensifier and 1024 channel linear detector used on the Doppler spectrometer.

tangential views through the plasma with tangency points from the plasma center to the edge. The operator can choose to keep the instrument on one spatial chord during one tokamak shot or repetitively scan across the whole set of 16 chords using a vibrating mirror. The instrument functions as a monochromator and uses a photomultiplier tube as a detector. In order to reduce random fluctuation, the photomultiplier output is filtered with a 3-msec RC time constant. Since the six-meter-long fiber-optic cables attenuate strongly at short wavelengths, the instrument is sensitive only to photons with wavelengths $\lambda \geq 2300$ Å.

The vuv monochromator has a 600-line/mm grating and usually is operated with 50-μm entrance and exit slits. It uses a continuous dynode electron multiplier for a detector and has a 3-msec filter on the output. The grating used with it permits detection of photons with wavelengths in the range $15 \text{ Å} \leq \lambda \leq 650$ Å.

B. Method of line identification

In order to search for and identify a magnetic dipole line in a given element, it is necessary to have a reasonably accurate prediction (usually ± 20 Å) of the wavelength of the line. Without this, the time it takes to make the search becomes too long and, even if a candidate line is found, the identification will remain necessarily uncertain. In principle, such predictions could be obtained from *ab initio* calculations (e.g., those of Cheng and Johnson for the Mg I sequence[18]). However, given the small energy level separations, *ab initio* calculations usually have insufficient accuracy, although recent calculations show significant improvement.[19] This accuracy can, of course, be improved by comparing with existing experimental results and adjusting some of the parameters in the calculations, as has been done for the $n=2$ levels.[20,21] Since corrections using experimental results are needed in any case, we have found it easier and more straightforward to utilize predictions based on isoelectronic fittings, such as those developed by Smit, Svensson, and Outred[22] for the Al I through Cl I sequence or by Curtis and Ramanujam[23] for the Mg I sequence. The formulas from Smit *et al.*[22] have been extrapolated to obtain the predictions needed for the Si I through S I sequences. The functional forms for the Mg I, Al I, and Cu I sequences are sufficiently simple that we have readjusted the fitting coefficients to take into account new data (e.g., from Hinnov *et al.*[7]) and thus produce better extrapolations.

If the wavelength range is suitable, the Doppler spectrometer is the preferred instrument, owing to its parallel multiwavelength detector. Necessary conditions for the identification of a line using this instrument are as follows: (1) the time behavior of the line after injection must match that of an electric dipole transition in the same ionization stage and, (2) the temperature inferred from the Doppler width must be reasonable for the given plasma conditions. Since the grating is most efficient near 12 000 Å, the line is sought first in the order which keeps the spectrometer setting near that wavelength. Once a candidate line is found, it is either observed in a different order or with the scanning visible instrument in first order to make sure that the initially assumed order was correct. An example of a spectrum of one of the newly identified lines is shown in Fig. 2.

If the wavelength for a candidate line is too long for the Doppler spectrometer, the line can still be sought using the scanning visible instrument. The search is considerably slower since the instrument only covers a 2-Å region of the spectrum per shot. The first criterion used for identification with the Doppler instrument is used here, too. Since no temperature can be determined, the identification relies heavily on having an identical time behavior of the magnetic and electric dipole lines. An example of this time behavior is shown in Fig. 3.

C. Wavelength determination

The wavelengths are measured according to a wavelength scale on the spectrometers. Consequently, the question of wavelength accuracy has two parts. First, how precisely can the wavelength of the line be determined relative to the local standard (i.e., spectrometer wavelength setting)? Second, how accurately can we relate the local standard to the absolute wavelength?

The precision of the measurements is determined as part of the fitting that is done to determine the centroid of the line. Both the Doppler and the scanning visible data can be used to generate a plot of line intensity versus

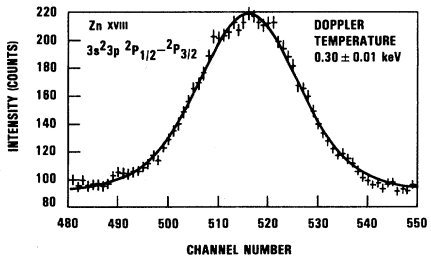

FIG. 2. Plot of a portion of the spectrum produced by the Doppler instrument for the Zn XVIII $3s^23p\ ^2P_{1/2}$-$^2P_{3/2}$ transition. Vertical bars show the error due to counting statistics. The continuous line is the result of the least-squares fit. The inferred temperature is 0.30±0.01 keV. χ^2 is 69.2 for 71 data points.

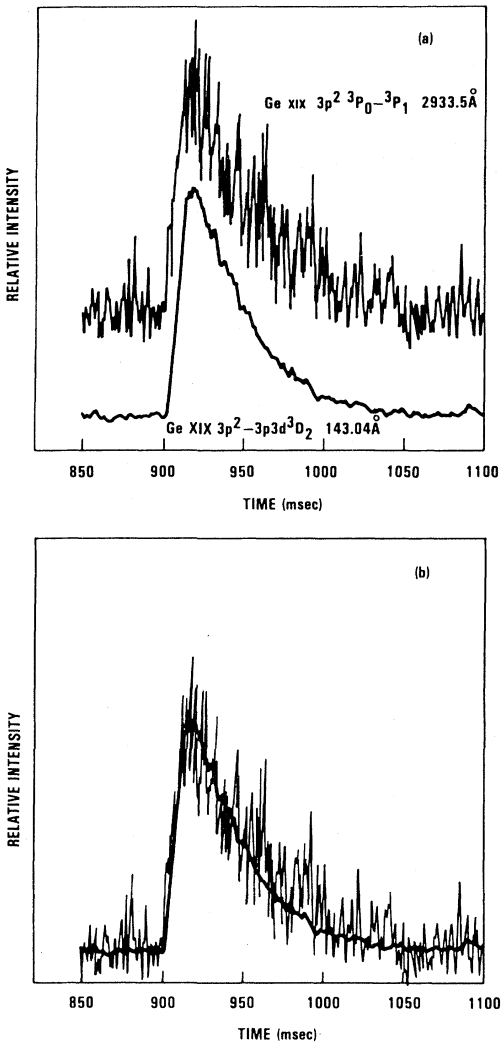

FIG. 3. (a) Time behavior of the Ge XIX electric dipole and magnetic dipole lines after germanium impurity injection. Time is given in ms after the start of the tokamak shot. (b) Illustration of how the time behaviors of the electric and magnetic dipole lines agree. The amplitude and background of the electric dipole line have been adjusted to best match, in a least-squares sense, the magnetic dipole line.

wavelength. Such a plot is trivially obtained from the Doppler data (see Fig. 2); the method used to produce it for the scanning visible data is presently described. The centroid is determined by fitting a functional form describing the line shape to the data using the Levenberg-Marquardt algorithm.[24,25] Such a nonlinear least-squares fit produces a value for the centroid and for the error in the centroid.[26]

For the Doppler system, the functional form used for the line shape is a convolution of the Gaussian Doppler profile emitted by the ion in the plasma with the measured instrumental response. (This response is determined by measuring the apparent shape of a very narrow line emitted by a mercury pen lamp.) Assuming that the error in each picture element of the 1024 channel detector is due to counting statistics, the χ^2 value of most of the fits is in the range of 50—100 for 100 data points, indicating quite a good fit. This fitting procedure produces values and errors for the ion temperature, line amplitude, and centroid location. Typically, the random error in the centroid location is ± 0.1 channels, which is smaller than the 0.5 channel error that one must ascribe to any detector system with discrete detectors. At 12 000 Å an error of ± 0.5 channels is equivalent to ± 0.06 Å.

The data taken with the scanning visible spectrometer can be used to build up a spectrum by scanning the wavelength on a shot-by-shot basis. Ideally, such data would be taken during a series of reproducible shots with an identical amount of impurity injected into each shot. However, since the tokamak shots are run for purposes other than spectroscopy, perfect reproducibility is not always attainable. In addition, while the gas injector is quite reproducible, the laser blowoff system exhibits about a 30% variation in the amount injected per shot. Variations in the injected amount can be compensated for by observing simultaneously both the candidate magnetic dipole line and an electric dipole line in the same ionization stage using the scanning visible and the vuv systems, respectively. Since the vuv wavelength is kept fixed while that of the scanning visible is varied, the ratio of the amplitudes of the two signals, plotted as a function of wavelength, can be used to produce a spectrum that is insensitive to variations in the amount of impurity injected. This method of normalization only works if the plasma density is not changing from shot to shot, since electric dipole line intensities respond linearly to plasma density variations, while magnetic dipole line intensities are independent of density except, possibly, due to cascade contributions.

The best way to calculate the ratio of amplitudes for a given shot is to treat the time varying scanning visible signal as the dependent variable y, the time varying vuv signal as the independent variable x, and then calculate the amplitude ratio as the slope of a y-x plot. Accurate values for the amplitude ratio and its error (owing to noise on the signal) can be obtained from a linear least-squares fit. In Fig. 3, one can see that, if the amplitude and background of the vuv signal are adjusted according to the results of the fit, the time behavior of the electric and magnetic dipole signals in Ge XIX is practically identical. In making such a linear fit, one must take care to exclude from the fit portions of the data which are contaminated by radiation from low ionization stages. Such portions are usually obvious due to the rapid onset of such radiation after impurity injection. For such cases, good data can be obtained from the decaying portion of the signal where the low ionization stage contribution has disappeared.

Once the amplitude ratio is known for each scanning visible wavelength setting, a fit can be done to these data to determine the line centroid. Such a fit is shown in Fig. 4. The fitting function used is a Gaussian plus background. The width of the line is simply due to instrumental broadening. From measurements with the mercury pen lamp, a Gaussian has been found to be an adequate fit to the instrumental profile. Typically, this fitting procedure yields random errors in the centroid position of 0.05 Å.

Having determined the line wavelength relative to our

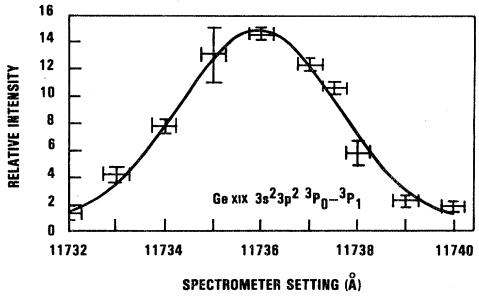

FIG. 4. Spectrum of the Ge XIX line plotted as a function of spectrometer setting. Owing to grating and order used, the actual wavelength is a quarter of the setting value. Horizontal error bars reflect the assumed ±0.2 Å reproducibility of the spectrometer setting; vertical bars represent the error in relative amplitude from the linear least-squares fit of data such as those in Fig. 3.

local standard still leaves us with the problem of determining the absolute wavelength. This requires calibrating the spectrometers by means of accurately known standards. For the Doppler and scanning visible spectrometers, this was done by using mercury lines,[27,28] whose wavelengths are quite precisely known. For the Doppler instrument, this calibration consists of making a table of the detector channel in which the centroid of each mercury line appears when the spectrometer is set at an integer multiple of the actual wavelength. Since the instrument is used with wavelength settings between 11 000 and 13 000 Å, fourth and fifth orders of various Hg I lines provide a reasonable number of calibration points. Scatter in the results based on multiple trials is used to determine the error in each centroid value. The actual first-order wavelength λ of the magnetic dipole line is related to the spectrometer setting λ_s by

$$\lambda=\frac{1}{n}\{\lambda_s+D(\lambda_s)[C-C_0(\lambda_s)]\}\ , \tag{1}$$

where D is the dispersion (in Å/channel), $C_0(\lambda_s)$ is the calibrated centroid value, C is the measured centroid value of the unknown line, and n is the spectrometer order. The wavelength calibration data $C_0(\lambda_s)$ are interpolated using cubic spline interpolation.[29] The dispersion is determined using close Hg I doublets;[27,28] these data are then fit to a functional form derived from the grating equation. The final random error in λ is determined by propagating the random error in λ_s, C_0, and all the calibration data through Eq. (1) using the usual formulas for random uncorrelated errors.[30]

The calibration data for the scanning visible instrument are a table of values of actual wavelength and spectrometer settings for the various mercury lines. The error in the spectrometer setting is determined by multiple trials or by the minimum instrumental accuracy (0.2 Å). Cubic spline interpolation is used for these data also. The random error in λ is found by propagating the error in λ_s and the calibration data through the spline formula (Ref. 29, Eq. 2.12).

The vuv calibration is based on a number of carbon, oxygen, and metallic impurity lines whose wavelengths are well known. These are emitted by ions in discharge cleaning plasmas, or in some cases, in actual tokamak shots. These data were analyzed by fitting to the grating equation and then using graphical interpolation on the deviations. Since we have only one vuv instrument, we lack a reference to smooth shot-to-shot variations in line intensity due to variations in the amount of impurity injected or in plasma conditions. Accordingly, a full numerical fit

TABLE I. Wavelengths for ions studied. Wavelengths above 2000 Å are in the air; square brackets denote tentative identifications.

Ion	Sequence	Transition	Wavelength (Angstroms) Present work	Other work
Zn XIV	Cl I	$3s^23p^5\,^2P^o_{3/2}$-$^2P^o_{1/2}$	2922.3±0.1[a]	
Zn XV	S I	$3s^23p^4\,^3P_2$-$^3P_1$	3450.4±0.2[b]	
Zn XVII	Si I	$3s^23p^2\,^3P_0$-$^3P_1$	[4355][b]	
		$3s^23p^2\,^3P_2$-$^1D_2$	2284.6±0.1[a]	
Zn XVIII	Al I	$3s^23p\,^2P^o_{1/2}$-$^2P^o_{3/2}$	2532.0±0.1[a]	
Zn XIX	Mg I	$3s3p\,^3P_1$-$^3P_2$	3296.2±0.2[b]	
Ge XVI	Cl I	$3s^23p^5\,^2P^o_{3/2}$-$^2P^0_{1/2}$	2084.9±0.1[a]	2085.1±0.1[c]
Ge XVII	S I	$3s^23p^4\,^3P_2$-$^3P_1$	2406.7±0.1[a]	2406.9±0.3[c]
				2406.5±0.5[d]
Ge XIX	Si I	$3s^23p^2\,^3P_0$-$^3P_1$	2933.5±0.1[b]	2933.7±0.2[c]
Ge XXI	Mg I	$3s3p\,^3P_1$-$^3P_2$	2350.0±0.1[a]	2350.2±0.3[c]
Se XIX	S I	$3s^23p^4\,^3P_1$-$^3P_0$	5593.9±0.6[b]	[5645.0][c]
Se XXI	Si I	$3s^23p^2\,^3P_2$-$3s^23p3d\,^3D_3$	129.7±0.5[e]	129.5±0.2[f]
		$3s^23p^2\,^3P_1$-$^3P_2$	4424.1±0.2[b]	4396.5±0.3[c]

[a]Doppler spectrometer measurement.
[b]Scanning visible spectrometer measurement.
[c]From Ref. 14.
[d]From Ref. 13.
[e]vuv spectrometer measurement.
[f]From Ref. 31.

and complete propagation of error analysis are not warranted here.

III. RESULTS

Our list of newly identified lines is given in Table I. We have taken advantage of further tokamak and calibration data to refine our previous wavelength measurements[11,15] and to improve our error estimates.

Some of our results can be compared with those of other workers. There has been considerable recent interest in germanium.[11,13,14] Where the same germanium line has been measured, the results in Table I agree with those of Roberts *et al.*[13] and Denne *et al.*[14] within the experimental error. The Se XXI $3s^2 3p^2\,{}^3P_2 - 3s^2 3p\,3d\,{}^3D_3$ electric dipole line has also been identified by Stratton *et al.*[31] at 129.5 ± 0.2 Å, which agrees with our measurement. There is a serious discrepancy between our values for the Se XIX and Se XXI magnetic dipole lines and those of Denne *et al.*;[14] further work to resolve this is necessary. As far as we know, there are no other zinc measurements with which we can compare.

IV. CONCLUSIONS

We have presented measured wavelengths for newly identified magnetic dipole transitions in the $n=3$ levels of ions of zinc, germanium, and selenium that were excited after being injected into tokamak plasmas in Doublet-III. These lines should aid in extending Doppler temperature and plasma rotation measurements to a broader range of plasma conditions. In addition, they will contribute to a fundamental knowledge of the energy-level structure of these ions.

ACKNOWLEDGMENTS

We would like to thank E. Hinnov, S. Suckewer, and B. Denne for communicating their data (Ref. 14) to us prior to publication and for several useful discussions. We also thank the Doublet-III tokamak physicists, especially the electron cyclotron heating group, for allowing us to piggyback on their experiments and to perturb the tail end of their shots. This work was supported by the U.S. Department of Energy under Contract DE-AT03-76ET51011.

[1] S. Suckerwer and E. Hinnov, Phys. Rev. Lett. 41, 756 (1978).
[2] S. Suckewer and E. Hinnov, Phys. Rev. A 20, 518 (1979).
[3] J. Lohr, C. J. Armentrout, G. Bramson, and P. Henline, Bull. Am. Phys. Soc. 25, 949 (1980).
[4] S. Suckewer, J. Cecchi, S. Cohen, R. Fonck, and E. Hinnov, Bull. Am. Phys. Soc. 25, 927 (1980).
[5] S. Suckewer, Phys. Scr. 23, 72 (1981).
[6] R. J. Groebner, A. J. Lieber, T. R. Angel, C. J. Armentrout, G. Bramson, K. H. Burrell, W. W. Pfeiffer, and F. B. Marcus, Bull. Am. Phys. Soc. 27, 959 (1982).
[7] E. Hinnov, S. Suckewer, S. Cohen, and K. Sato, Phys. Rev. A 25, 1101 (1982).
[8] S. Suckewer, H. P. Eubank, R. J. Goldston, E. Hinnov, and N. R. Sauthoff, Phys. Rev. Lett. 43, 207 (1979).
[9] S. Suckewer, H. P. Eubank, R. J. Goldston, J. McEnerey, N. R. Sauthoff, and H. H. Towner, Nucl. Fusion 21, 1301 (1981).
[10] R. C. Isler, L. E. Murray, E. C. Crume, C. E. Bush, J. L. Dunlap, P. H. Edmonds, S. Kasai, E. A. Lazarus, M. Murakami, C. H. Neilson, V. K. Paré, S. D. Scott, C. E. Thomas, and A. J. Wooten, Nucl. Fusion 23, 1017 (1983).
[11] K. H. Burrell and R. J. Groebner, Bull. Am. Phys. Soc. 27, 1100 (1982).
[12] S. Suckewer, E. Hinnov, S. Cohen, M. Finkenthal, and K. Sato, Phys. Rev. A 26, 1161 (1982).
[13] J. R. Roberts, V. Kaufman, J. Sugar, T. L. Pittman, and W. L. Rowan, Phys. Rev. A 27, 1721 (1983).
[14] B. Denne, E. Hinnov, S. Suckewer, and S. Cohen, Phys. Rev. A 28, 206 (1983).
[15] K. H. Burrell, R. J. Groebner, and N. H. Brooks, Bull. Am. Phys. Soc. 28, 921 (1983).
[16] J. F. Friichtenicht, Rev. Sci. Instrum. 45, 51 (1974).
[17] S. C. Bates and K. H. Burrell, GA Technologies Inc. Report No. GA-A17055 (unpublished).
[18] K. T. Cheng and W. R. Johnson, Phys. Rev. A 16, 263 (1977).
[19] D. Frye, S. Lakdawala, and L. Armstrong, Jr., Phys. Rev. A 27, 1709 (1983).
[20] B. Edlén, Phys. Scr. 26, 71 (1982).
[21] K. T. Cheng, Y. K. Kim, and J. P. Desclaux, At. Data Nucl. Data Tables 24, 111 (1979).
[22] R. Smit, L. A. Svensson, and M. Outred, Phys. Scr. 13, 293 (1976).
[23] L. J. Curtis and P. S. Ramanujam, Phys. Scr. 23, 1043 (1981).
[24] K. Levenberg, Q. Appl. Math. 2, 164 (1944).
[25] D. W. Marquardt, J. SIAM 11, 431 (1963).
[26] P. R. Bevington, *Data Reduction and Error Analysis for the Physical Sciences* (McGraw-Hill, New York, 1969), p. 242.
[27] V. Kaufman and B. Edlén, J. Phys. Chem. Ref. Data 3, 825 (1974).
[28] K. Burns, K. B. Adams, and J. Longwell, J. Opt. Soc. Am. 40, 339 (1950).
[29] J. H. Ahlberg, E. N. Nilson, and J. L. Walsh, *The Theory of Splines and Their Applications* (Academic, New York, 1967), Chaps. 1 and 2.
[30] Reference 26, Chap. 4.
[31] B. C. Stratton, W. L. Hodge, H. W. Moos, J. L. Schwob, S. Suckewer, M. Finkenthal, and S. Cohen, J. Opt. Soc. Am. 73, 877 (1983).